View metadata, citation and similar papers at core.ac.uk
brought to you by CORE
provided by Brunel University Research Archive

2nd Micro and Nano Flows Conference
West London, UK, 1-2 September 2009

Blood Flow in Microvascular Networks

Mohamed H. MANSOUR [1], Neil W. BRESSLOFF[1,*], Cliff P. SHEARMAN [2]

* Corresponding author: Tel.: ++44 (0)2380595473; Fax: ++44 (0)2380594813; Email: N.W.Bressloff@soton.ac.uk
1: School of Engineering Sciences, University of Southampton, Highfield, Southampton, SO17 1BJ, U.K.
2: Department of Vascular Surgery, Southampton General Hospital, Southampton, SO16 6YD, U.K.

Abstract Simulation of blood presents a very complex haemodynamics problem especially in relation to the understanding of atherogenesis. In many simulations, blood has been treated as a single-phase homogeneous fluid, a classical approach that does not account for the presence of red blood cells (RBCs). Although this approach provides satisfactory tools to describe certain aspects of blood flow in large arteries, it fails to give an adequate representation of the flow field in the vessels of smaller diameter where the size of the RBC becomes significant relative to vessel diameter. So, this article is concerned with the study of non-Newtonian blood flow in microvascular networks with the intention of developing a new cell depletion layer model to represent the behaviour of RBCs through bifurcating networks. The model is tested in a microvascular network constructed possessing realistic bifurcation features, with controlled dimensions and angles. The RBC depletion model treats blood as two continuum layers, with a central, non-Newtonian core region of concentrated red cell suspension that is surrounded by a layer of plasma (Newtonian fluid) adjacent to the vessel wall. In the central core region, blood is described by Quemada's non-Newtonian rheological model. Geometry differences are shown to significantly affect flow rates, haematocrit distributions and the corresponding cell depletion layers.

Keywords: Non-Newtonian, microvascular, Network, Red blood cell depletion model, Quemada model

1. Introduction

In microvessels (20-500 microns in diameter), there are two key processes influencing the flow of blood. The first concerns the aggregation of RBCs resulting from shear rates that are small enough to enable red blood cells to form aggregate structures of varying sizes and morphology. This aggregation may be formed when the cells come into close proximity. One explanation often advanced for aggregation is the bridging hypothesis, which postulates that long-chain macromolecules such as fibrinogen or dextrans of high molecular weight may be adsorbed onto the surface of more than one cell, leading to a bridging effect between cells. It has been proposed by other investigators that the reduced concentration of macromolecules in the vicinity of red cells lowers the osmotic forces in the vicinity, causing fluid to move away and increasing the tendency for adjacent red cells to come together. According to both the bridging and the depletion theories, the total adherent force between two cells is maximal when the cells are oriented en face, thus it is not uncommon to observe cells arranged in rouleaux, Bishop *et al.* (2001).

The second process results from shear rate gradients, which create a force that counteracts dispersion forces and tends to move red cells and aggregates away from the vessel wall, Bishop *et al.* (2001). This radial migration of red blood cells leads to the formation of a cell-depleted layer at the vessel wall.

The aggregation of red blood cells in blood flowing through small tubes leads to the two-layer flow of an inner core of rouleaux surrounded by a cell-depleted peripheral layer, [Bagchi (2007), Srivastava (2007), Das *et al.* (2000), Das *et al.* (1997), Sharan & Popel (2001), Cokelet & Goldsmith (1991), Chen *et al.* (2006) and Kim *et al.* (2007)]. The formation of this layer is known to be accompanied by a decrease in hydrodynamic resistance to flow.

Furthermore, the size and distribution of the aggregates affect the flow impedance in a way that may be characterized by an "apparent viscosity". Effectively, when aggregates migrate to the centre of the vessel, particle size is greater in the centre than near the wall, and so the effective viscosity is greater in the centre as well. Thus, the net effect of aggregation on effective blood viscosity creates two opposing tendencies, increased viscosity in the centre due to increased particle size and decreased viscosity near the wall due to reduced haematocrit.

In microvessel networks, the processes described above are superimposed on the flow produced by bifurcations. Typically, a disproportionate fraction of red blood cells generally flows into the branch that receives a higher total flow leading to a higher haematocrit (the proportion of blood volume that is occupied by red blood cells) in that branch than in the other. In particular, if the flow into the low flow branch is sufficiently small, RBCs do not enter that branch. Effectively, the low flow branch skims plasma from the peripheral layer of the flow. Such behavior reflects axial migration of RBCs upstream of the bifurcation, producing a phase separation in the parent vessel, and this physiological phenomenon, which causes heterogeneity in the microcirculation, is caused by a cell-depleted wall layer. The fluid forces at a bifurcation can also affect phase separation. Since blood cells are finite size particles, a certain fraction of them will always be found along the dividing stream surface. Only at the branch point the balance of fluid forces will determine which way such cells go, leading to a partial separation of the solid and fluid phase. This process does not require an uneven distribution of the haematocrit in the parent vessel, and is called red cell screening, Shibeshi and Collins (2005).

In the presence of red blood cell aggregation, velocity profiles become blunted as pseudo-shear rate (= mean fluid velocity/vessel diameter) is decreased from ~ 100 s^{-1} to 5 s^{-1}. Also, there is *in vivo* evidence that the short distance between channel junctions in venules does not appear to permit significant radial migration and red cell depletion of the peripheral fluid layer between bifurcations, and that the formation of a cell-depletion plasma layer at the vessel wall only occurs at very low pseudo-shear, Bishop *et al.* (2001).

Whilst the lattice-Boltzmann method has been successfully used to model individual RBCs flowing through relatively simple blood vessels, it is likely that application to more complex geometry would be prohibitively expensive. Thus, a mathematical model is described here to capture the affects described above and which can be sensibly applied to microvascular networks. Cell depletion effects are simulated by a two-layer model in which the haematocrit and viscosity are tightly coupled.

2 Quemada model for two-layer blood flow

A number of constitutive models have been proposed to describe the bulk rheological behavior of blood. Among these, the Casson model has been most widely used. Quemada extended the Casson model using first physical principles and explicitly described the kinetics of RBC aggregation; this model includes a structural parameter, which is related to the size of RBC aggregates. As a result, the viscosity is not infinite at zero shear rates in the Quemada model making it attractive for modeling blood flow in microvessels. Also, the Quemada model accurately fits experimental viscometric data for small diameter vessels (above 12 μm diameter), Das *et al.* (1997). The viscosity results for this model lie between the *in vitro* and *in vivo* values. The Quemada model is thus used to model the central core of RBC suspensions whilst the peripheral plasma layer is modeled as a Newtonian fluid.

3 Mathematical model

Consider a RBC depletion model for blood flow within a cylindrical tube of radius R consisting of a central core of radius r_c and effective viscosity μ_c, which contains a suspension of plasma and red blood cells, and a cell-depleted layer outside the core containing plasma with an effective viscosity, μ_p. This model is also called a two-layer model because the flow consists of two layers of different

fluids. Fig. (1) is an idealized representation of the cell-depletion model when the cell depletion layer is fully developed.

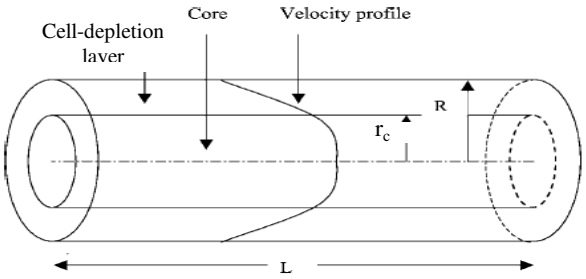

Fig. (1) Blood flow in a cylindrical tube modeled by a RBC depletion model

3.1 Governing equations

The mass and momentum conservation equations for an incompressible fluid can be written as

$$\nabla . V = 0 \tag{1}$$

$$\rho\left(\frac{\partial V}{\partial t} + V.\nabla V\right) = -\nabla p + \nabla.\tau \tag{2}$$

where, ρ, V, p, τ denote the density, the velocity field, the pressure and the deviatoric stress tensor, respectively. This tensor is related to the viscosity and the shear rate tensor according to the relation

$$\tau = \mu(\dot{\gamma})D \tag{3}$$

where the viscosity, $\mu = \begin{cases} \mu_p & r_c \le r \le R \\ \mu_c & 0 \le r \le r_c \end{cases}$, is a function of the shear rate $\dot{\gamma}$ and the shear rate tensor D at the core region. The relation between the shear rate and the shear rate tensor is expressed as

$$\dot{\gamma} = \sqrt{\frac{1}{2}\sum_i\sum_j D_{ij}D_{ji}} \tag{4}$$

and,

$$D = \begin{bmatrix} \frac{\partial u}{\partial x} & \frac{1}{2}\left(\frac{\partial u}{\partial y} + \frac{\partial v}{\partial x}\right) & \frac{1}{2}\left(\frac{\partial u}{\partial z} + \frac{\partial w}{\partial x}\right) \\ \frac{1}{2}\left(\frac{\partial u}{\partial y} + \frac{\partial v}{\partial x}\right) & \frac{\partial v}{\partial y} & \frac{1}{2}\left(\frac{\partial w}{\partial y} + \frac{\partial v}{\partial z}\right) \\ \frac{1}{2}\left(\frac{\partial u}{\partial z} + \frac{\partial w}{\partial x}\right) & \frac{1}{2}\left(\frac{\partial w}{\partial y} + \frac{\partial v}{\partial z}\right) & \frac{\partial w}{\partial z} \end{bmatrix} \tag{5}$$

The shear rate is, therefore, calculated in Cartesian coordinates as

$$\dot{\gamma} = \left[2\left\{(\partial u/\partial x)^2 + (\partial v/\partial x)^2 + (\partial w/\partial x)^2\right\} + (\partial u/\partial z + \partial w/\partial x)^2 + (\partial u/\partial y + \partial v/\partial x)^2 + (\partial v/\partial z + \partial w/\partial y)^2\right]^{1/2} \tag{6}$$

The viscosity is related to the structural parameter (k) and the blood local haematocrit H, according to the Quemada model in the form

$$\mu_c = \mu_p \frac{1}{(1 - 0.5kH)^2} \tag{7}$$

The rheological model proposed by Quemada considers blood as a structured fluid, wherein the state of RBC aggregation is described by the structural parameter k, which characterizes the average number of RBCs in an aggregate.

$$k = \frac{k_0 + k_\infty\sqrt{\dot{\gamma}/\gamma_c}}{1 + \sqrt{\dot{\gamma}/\gamma_c}} \tag{8}$$

where, k_0 and k_∞ are the intrinsic viscosities at zero and infinity shear rates, respectively, of the flow particles which predominate at those shear rates. γ_c signfies the critical shear rate, which can be considered to be the inverse of the relaxation time for the dominant structural unit causing the suspension to be non-Newtonian. Here, k_0, k_∞ and γ_c are functions of H, Cokelet (1987).

$$k_0 = \exp(3.8740 + H(-10.41 + H(13.8 - 6.738H))) \tag{9}$$

$$k_\infty = \exp(1.3435 + H(-2.803 + H(2.711 - 0.6479H))) \tag{10}$$

$$\gamma_c = \exp(-6.1508 + H(27.923 + H(-25.6 + 3.697H))) \tag{11}$$

The distribution of haematocrit is simulated by a conservation equation describing the transport of haematocrit and encapsulating the behaviour of RBCs in blood flowing through bifurcating networks. The conservation equation employs convection and diffusion terms according to

$$(\rho V_{RBC}.\nabla)H - \nabla(\Gamma\nabla H) = 0 \tag{12}$$

where ρ, V_{RBC}, H and Γ are the density, RBC

velocity field, haematocrit and the diffusion coefficient, respectively.

Following Rudman (1997), V_R is computed from

$$V_{RBC} = V_{bulk} - (1 - 6.55H)\frac{(\rho - \rho_{RBC})}{\rho K}\nabla.\bar{\sigma} \quad (13)$$

V_{bulk}, K, ρ_{RBC} and $\bar{\sigma}$ denote, respectively, the bulk velocity of the flow, the coefficient that represents the drag force between red blood cells, the density of a red blood cell and the stress tensor.

$$K = (9\mu)\Big/(2a^2) \quad (14)$$

where a is the red blood cell radius and is equal to 3.5 μm. The stress tensor is evaluated from

$$\Delta.\bar{\sigma} = -\nabla p + \nabla.\tau \quad (15)$$

The haematocrit diffusion coefficient, Γ, can be calculated, Scott (2005), by adding a fluctuating term arising from collisions with solvent molecules and with other particles to the Einstein-Stokes diffusion constant, Γ_0,

$$\Gamma = \Gamma_0(1 - a_1\varepsilon H) \quad (16)$$

ε is a Peclet number, and measures the ratio of the magnitude of the convective flux to the magnitude of the diffusive flux.

$$\Gamma_0 = \frac{K_p T}{6\pi\mu_p a} \quad (17)$$

where K_p and T are Boltzmann's constant and the absolute temperature, respectively.

$$\varepsilon = \frac{11}{140}\frac{V^2}{\alpha}\frac{\mu_p a}{\Gamma_0}\left(\frac{a}{R}\right)^2 = \frac{11}{140}\frac{V^2}{R^2}\frac{\mu_p a^3}{\Gamma_0\alpha} \quad (18)$$

$$\approx \frac{11}{140}\dot{\gamma}^2\frac{\mu_p a^3}{\Gamma_0\alpha} \quad (19)$$

Alternatively, the parameter ε can be thought of as a measure of the inhomogeneity of the particle distribution, since ε = 0 corresponds to the diffusion dominated regime, and therefore to a homogeneous particle distribution. α is the interfacial tension and equal to 1.24×10^{-4} N m^{-1}. Also, a_1 is determined from experiments, Scott (2005). It has a constant value of 3.77. The results of Eqn. (16) were compared with previous experimental results by Scott (2005) as shown in Fig. (5.7) in his thesis and the results obtained were in good agreement with others. It is important to note that the shear-induced diffusion is a function of the shear rate and the viscosity, which are exist in the definition of the parameter (ε). So, the effect of the shear-induced migration is concluded in ε.

4 Numerical procedure

A theoretical model has been developed to simulate blood flow through microcirculatory networks with vessel diameters in the range of 20-500μm. The model takes into account the dependence of apparent viscosity of blood on shear rate, haematocrit and structural parameter (k), the reduction of intravascular haematocrit relative to the inflow haematocrit of a vessel, and the disproportionate distribution of red blood cells and plasma at arteriolar bifurcations (phase separation). The cell depletion model is used to simulate flow in a microvascular network, constructed from experimental data (length, diameter, and blood velocity) obtained from Scott (2005) and Gentile *et al.* (2008). Haematocrit and velocity distributions in all vessel segments of this network are calculated.

The algorithm described above is coded as a set of user defined functions in Fluent (Ansys), which are applied in three stages in order to obtain convergence. At first, initial values for the velocity field, haematocrit and the viscosity are applied. The viscosity and the diffusion coefficient of the scalar transport equation are set constant, and V_R is set equal to the flow velocity field. Then, the continuity and momentum equations are solved followed by the scalar conservation equation for H to yield new values of the velocity field and H. These are used again to calculate more accurate values of V and H. This procedure is repeated for 200 iterations since it was found that, without this step, μ could not be suitably initialised. In the second step of the solution, the viscosity is kept constant whilst the diffusion coefficient and the RBC velocity are calculated as described above. Finally, in the third step of the solution, the viscosity is evaluated from k and H, first by calculating k from Eq. 8. This iterative procedure is repeated until convergence is achieved (when the mean

residuals of the continuity, momentum and haematocrit equations reach stable constant values).

The setup in Fluent comprises the implicit pressure based solver with second order velocity and pressure interpolation, and the Green-Gauss cell based method for gradients.

5 Network construction

The network used in this study (c.f. Figure 2) was constructed using a new technique in which an in-house C-code was used to generate an VBS format input file for CATAIA V5 (Dassault Systemes) containing appropriate sectional information based on the required geometry of the network.

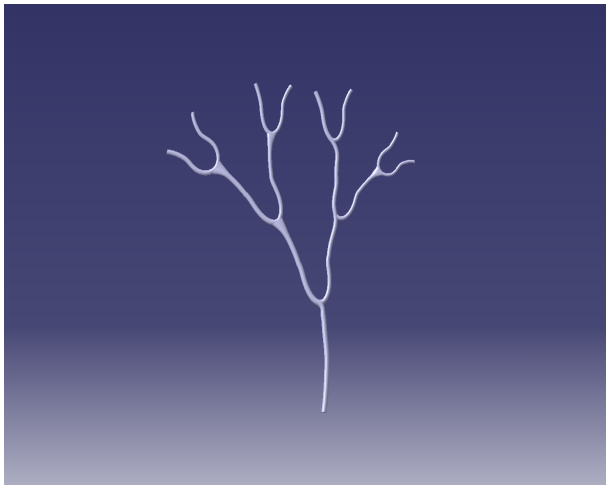

Fig. (2) The geometry of the network

Whilst it is recognized that there is often a desire to perform simulations through realistic arteriole networks, the approach developed here provides a flexible automated method for generating a range of representative networks possessing realistic geometric features. These particularly include the different ways that segments bifurcate. In this method, the first bifurcation is defined, as shown in Table 1, and then the network is effectively grown in a quasi-random way such that the diameter and angle of each bifurcation are selected by random numbers varying between appropriate ranges: the diameter values vary between 50 and 100 μm and the outlet angle values range between 10º and 60º.

Parent branch diameter	100 μm
First daughter branch diameter	80 μm
First daughter branch outlet angle	30º
second daughter branch diameter	90 μm
second daughter branch outlet angle	-20º

Table (1). The dimensions of the first bifurcation of the microvascular network.

6 Boundary conditions

To simulate blood flow through the microvascular network of this study, it is necessary to specify flow rates or pressures both at the inlet and outlets of the network. Information to specify the flow rate at the outlet branches of the network could not be found in the literature and so the pressure is fixed at the inlet to 300 Pa and to 0 Pa at the eight outlets. These values yield mean axial velocities in these branches with values similar to those available in the literature. Also, the blood haematocrit at the inlet has a constant value of 0.4. At the outlet, the haematocrit gradient is zero. Finally, at the wall, all the values of the velocity and the haematocrit are equal to zero.

7 Mesh study

A mesh dependence study was performed on the network to determine a suitable grid resolution. The velocity distributions were observed at the inlet, and the outlets of the network for three different cell sizes: 2, 3 and 4μm. These resolutions were selected since it was found that convergence could not be obtained on coarser grids. The effect of the cell size is small at the inlet but it is greater at the outlet. It is to be noted that the velocities at the outlets of the 2 and 3 micron grids differ by up to 3 %. Nonetheless, with a view towards future studies, it was decided to limit the cell count to less than five million cells, and so a cell size of 3 microns (and 4445624 cells) was deemed to be suitable for the network.

8 Results

Blood flow simulations were performed on the network using the red blood cell depletion model with a pressure difference of 300 Pa as described above. Fig. 3 depicts the haematocrit on the symmetry plane. A cell depletion layer develops downstream from the inlet and persists on the outer walls through to outlets 1 and 8. This characteristic is evident at all

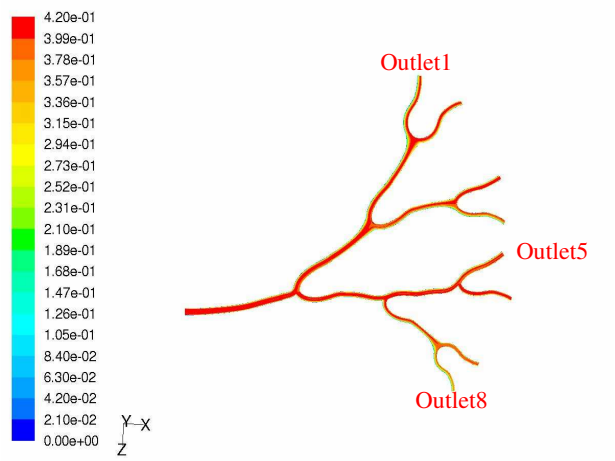

Fig. (3) The haematocrit contour at the symmetry plane of the network

bifurcations whereby the cell depletion layer that develops in the upstream segment persists on the outer wall. Furthermore, the core fluid that impinges on the flow divider (with relatively high haematocrit) also develops a depletion layer, but this is thinner than on the corresponding outer wall. Ultimately, successive bifurcations then lead to the asymmetric haematocrit distributions at the outlets shown in Figs. (4-9). The three outlets considered are labeled in Fig. (3).

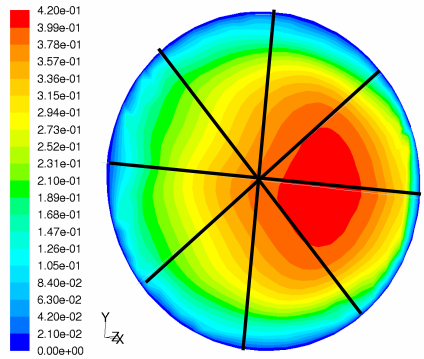

Fig. (4) Haematocrit distribution (outlet 1).

In Fig. (4), the haematocrit shows strong asymmetry along line L1, aligned with the symmetry plane. This is in agreement with findings elsewhere, Carr and Wickham (1990), and is further emphasized in Fig. (5) in which the haematocrit profiles along lines L1, L2, L3 and L4 are depicted.

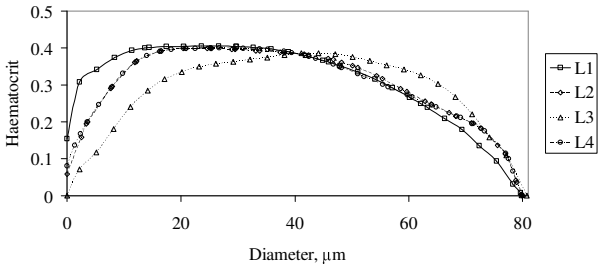

Fig. (5) Haematocrit profiles (outlet 1).

Less asymmetry is evident in the central vessels, as shown by way of example for outlet 5 in Figs. (6) and (7). Indeed, this outlet lies at the end of the straightest path through the network and, as a result, it has a haematocrit distribution with a distinct, relatively constant, core region (c.f. Fig. (7)).

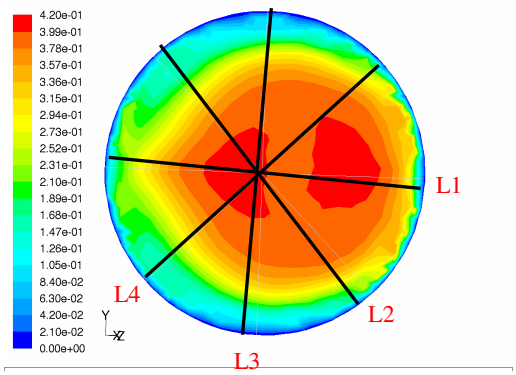

Fig. (6) Haematocrit distribution (outlet 5).

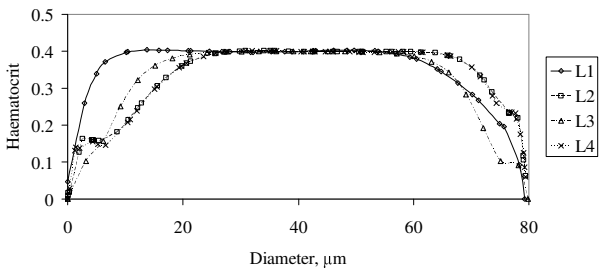

Fig. (7) Haematocrit profiles (outlet 5).

Finally, the haematocrit distribution and corresponding profiles are shown in Figs. (8) and (9), respectively. Due to outlets 1 and 8

lying on the outermost paths through the network, it would seem that similar asymmetry is evident in both outlets. However, the diameter of outlet 8 is smaller (50 microns) than that of outlet 1 (80 microns). Also, the upstream bifurcations for each outlet are different; in particular, the second bifurcation upstream of outlet 8 represents more of a side branch compared to the equivalent bifurcation

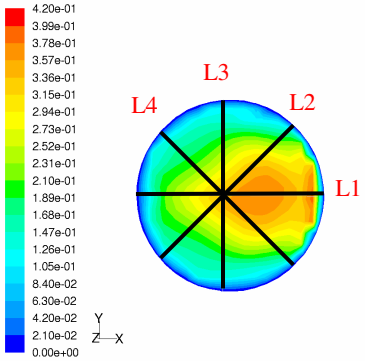

Fig. (8) Haematocrit distribution (outlet 8).

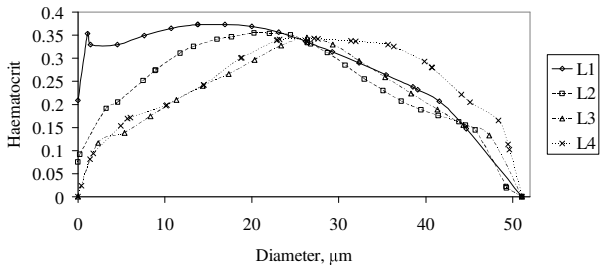

Fig. (9) Haematocrit profiles (outlet 8).

for outlet 1. These geometric differences produce different flow rates in each branch (the flow rate is approximately five times higher through outlet 1 than outlet 8), and hence the magnitude of the haematocrit is less in outlet 8 than that in outlet 1. Jafari *et al.* (2006) found a similar correlation between flow rate and haematocrit.

It is clear from the results above that there is significant variation between haematocrit profiles both within a single branch and in different branches. Consequently, it is difficult to define the cell depletion layer in all outlets. Indeed, of the outlets considered here, a cell depletion layer thickness can only be meaningfully defined for the haematocrit distribution in outlet 5. Here, it is assumed that the cell depletion layer thickness, δ, is defined as the width of the flow when the value of the haematocrit reaches 99% of the maximum haematocrit at that section. If δ is computed along lines L1, L2, L3 and L4, the average cell-depletion layer thickness is found to equal 0.578R.

Evidently, repeated bifurcations dramatically influence haematocrit distributions, profiles and the corresponding cell depletion layer. For a straight vessel (with the same radius as outlet 5) Bagchi (2007) calculated the value of the cell-depletion layer thickness to be 0.1R.

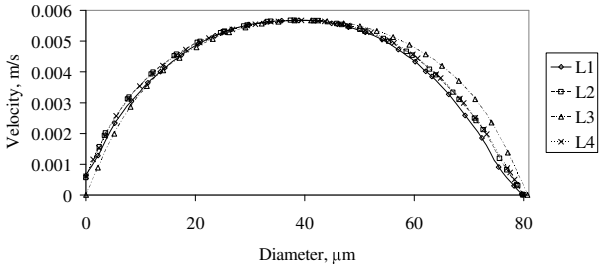

Fig. (10) Velocity profiles (outlet 1).

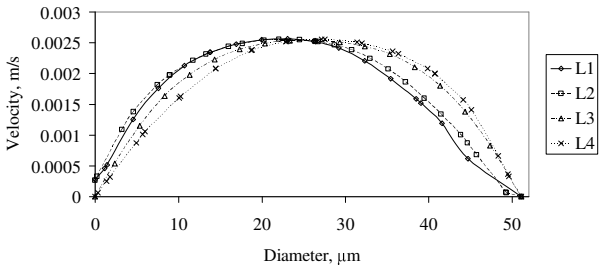

Fig. (11) Velocity profiles (outlet 8).

The velocity profiles for outlets 1 and 8, shown in Figs. (10) and (11), are relatively blunt (a feature that is associated with accumulation of blood cells along the axis of the vessel). Also, greater asymmetry in the flow is observed for the eighth outlet due to the bifurcating effect discussed above.

9 Conclusions

A theoretical cell depletion model has been developed to simulate blood flow through arteriole networks. The model takes into account the dependence of the viscosity of the blood on the structure parameter and the haematocrit. A new expression for calculating the diffusion coefficient as a function of the flow conditions and red blood cell properties is introduced to take into account the forces

acting on a deformable particle in tube flow. The migration velocity of the RBCs is computed and applied to this haematocrit conservation equation to develop the core region. The model was used to simulate blood flow in a representative microvascular network. The reduction of intravascular haematocrit relative to the inflow haematocrit of a vessel, and a representation of the disproportionate distribution of red blood cells and plasma at arteriolar bifurcations (phase separation) are observed. It is clear that the geometry of repeatedly bifurcating arteriole segments dramatically affects the distribution of haematocrit. A blunt haematocrit distribution is only observed in outlet branches lying at the end of a relatively straight path through the network, and it is only in such locations that a meaningful cell depletion layer thickness can be defined. Even so, the thickness is significantly larger than that in straight vessels. Also, the geometry influences flow rates which, in turn, affect haematocrit magnitude.

Finallly, the results also show that the velocity profile for the red blood cell depletion model is not parabolic but takes a blunted shape. This is due to modeling of the accumulation of blood cells along the axis of the vessels.

References

Bagchi, P., 2007. Mesoscale Simulation of blood flow in small vessels. Biophysical Journal. 92, 1858-1877.

Bishop, J. J., Popel, A. S., Intaglietta, M., and Johnson, P. C., 2001. Rheological effects of red blood cell aggregation in the venous network: A review of recent studies. Biorheology. 38, 263–274.

Carr, R. T., and Wickham, L. L., 1990. Plasma Skimming in Serial Microvascular Bifurcations, Microvascular Research, 40, 179–190.

Chen, X., Jaron, D., Barbee K. A., and Buerk, D. G., 2006. The influence of radial RBC Ddstribution, blood velocity profiles and coupled NO/O_2 transport. J. Appl. Physiol. 100, 482–492.

Cokelet, G. R., 1987. The Rheology and Tube Flow of Blood. In: Handbook of Bioengineering, edited by R. Skalak and S. Chien. New York: McGraw Hill. 14.1-14.17.

Cokelet, G.. R., and Goldsmith, H. L., 1991. Decreased hydrodynamic resistance in the two-phase flow of blood through small vertical tubes at low flow rates. Circ. Res. 68, 1–17.

Das, B., Enden, G.., and Popel, A. S., 1997. Stratified multiphase model for blood flow in a venular bifurcation. Annals of Biomedical Engineering. 25, 135–153.

Das, B., Johnson, B. C., and Popel, A. S., 2000. Computational fluid dynamic studies of leukocyte adhesion effects on non-Newtonian blood flow through microvessels. Biorheology. 37, 239–258.

Gentile, F., Ferrari, M., and Decuzzi, P., 2008. The transportation of nanoparticles in blood vessels: the effect of vessel permeability and rheology. Annals of Biomedical Engineering. 36, 254–261.

Jafari, A., Mousavi, S. and Kolari, P., 2006. Numerical investigation of blood flow. Part I: In Microvessel Bifurcations. Communication in Nonlinear Science and Numerical Simulation, 13 (8), 1615-1626.

Kim, S., Kong, R. L., Popel, A. S., Intaglietta, M., and Johnson, P. C., 2007. Temporal and spatial variations of cell-free layer width in arterioles. Am. J. Physiol Heart Circ. Physiol. 239, H1526–H1535.

Rudman, M., 1997. One-Field Equations for Two-Phase Flows. J. Austral. Math. Soc. Sep. B 39, 149-170.

Scott, M., 2005. The modeling of blood rheology in small vessels, A thesis for the degree of doctor of philosophy in applied mathematics. Waterloo, Ontario, Canada.

Sharan, M., and Popel, A. S., A, 2001. Two-phase model for flow of blood in narrow tubes with increased effective viscosity near the wall. Biorheology. 38, 415–428.

Shibeshi, S., and Collins, W., 2005. The rheology of blood flow in a branched arterial system. Appl. Rheol. 15, 398-405.

Srivastava, V. P., A, 2007. Theoretical model for blood flow in small vessels. Applications and Applied Mathematics. (AAM). 2 (1), 51–65.